Methylation of tRNA^{Asp} by the DNA Methyltransferase Homolog Dnmt2

Mary Grace Goll,[1] Finn Kirpekar,[2] Keith A. Maggert,[3] Jeffrey A. Yoder,[4] Chih-Lin Hsieh,[5] Xiaoyu Zhang,[6] Kent G. Golic,[7] Steven E. Jacobsen,[6] Timothy H. Bestor[1]*

The sequence and the structure of DNA methyltransferase-2 (Dnmt2) bear close affinities to authentic DNA cytosine methyltransferases. A combined genetic and biochemical approach revealed that human DNMT2 did not methylate DNA but instead methylated a small RNA; mass spectrometry showed that this RNA is aspartic acid transfer RNA (tRNA^{Asp}) and that DNMT2 specifically methylated cytosine 38 in the anticodon loop. The function of DNMT2 is highly conserved, and human DNMT2 protein restored methylation in vitro to tRNA^{Asp} from Dnmt2-deficient strains of mouse, *Arabidopsis thaliana*, and *Drosophila melanogaster* in a manner that was dependent on preexisting patterns of modified nucleosides. Indirect sequence recognition is also a feature of eukaryotic DNA methyltransferases, which may have arisen from a Dnmt2-like RNA methyltransferase.

The DNA (cytosine 5) methyltransferases of the Dnmt1 and Dnmt3 families establish and maintain patterns of methylation at cytosine residues in flowering plants, deuterostomes, and a subset of protostomes (*1*). Proteins of the Dnmt2 family show all the sequence and structural characteristics of DNA methyltransferases (*2*–*5*) except for a putative nucleic acid binding cleft that cannot easily accommodate duplex DNA (*1*). Despite the sequence and structural affinities between Dnmt2 and authentic DNA methyltransferases, genomic methylation patterns are not measurably altered in Dnmt2-deficient mouse embryonic stem (ES) cells (*6*).

Localization experiments indicate that Dnmt2 does not have the properties expected of a DNA methyltransferase. Human DNMT2 protein (hDNMT2) is primarily localized to the cytoplasm of transfected mouse 3T3 fibroblasts (Fig. 1). The cytoplasmic localization of DNMT2 contrasts with the exclusively nuclear localization of Dnmt1 and Dnmt3 (*7*, *8*).

The biological function of Dnmt2 was evaluated in strains of mouse, *Arabidopsis thaliana*, and *Drosophila melanogaster* that lack Dnmt2 (Fig. 2). The mouse deletion allele excised amino acids 181 to 359; this region includes the highly conserved Cys-Phe-Thr-XX-Tyr-XX-Tyr (where X is any amino acid) motif unique to Dnmt2 homologs (*1*, *4*) and DNA cytosine methyltransferase motifs VIII and IX (Fig. 2A and fig. S1). The *MT2*/*Dnmt2* (hereafter *dDnmt2*) gene of *D. melanogaster* was disrupted by insertion of 28 base pairs of sequence that contained three in-frame stop codons and a +1 frameshift 5′ of the region that encodes motif IV (Fig. 2B), which is required for enzymatic activity (*9*). Wild-type *Dnmt2* sequence was not present in flies homozygous for this mutation (fig. S2). A strain of *A. thaliana* that contains a large *Agrobacterium* transferred DNA (T-DNA) insertion adjacent to exon 7 (Fig. 2C) was obtained from the Salk T-DNA collection (*10*). The introduction of deletion or truncating mutations in all three organisms causes loss of catalytic motifs that

[1]Department of Genetics and Development, College of Physicians and Surgeons, Columbia University, New York, NY 10032, USA. [2]Department of Biochemistry and Molecular Biology, University of Southern Denmark, Campusvej 55, DK-5230 Odense M, Denmark. [3]Department of Biology, Texas A&M University, College Station, TX 77843, USA. [4]Department of Molecular Biomedical Sciences, College of Veterinary Medicine, North Carolina State University, Raleigh, NC 27606, USA. [5]Department of Urology and Department of Biochemistry and Molecular Biology, University of Southern California, Los Angeles, CA 90089, USA. [6]Howard Hughes Medical Institute (HHMI) and Department of Molecular, Cell, and Developmental Biology, University of California, Los Angeles, CA 90095, USA. [7]Department of Biology, University of Utah, Salt Lake City, UT 84112, USA.

*To whom correspondence should be addressed. E-mail: THB12@Columbia.edu

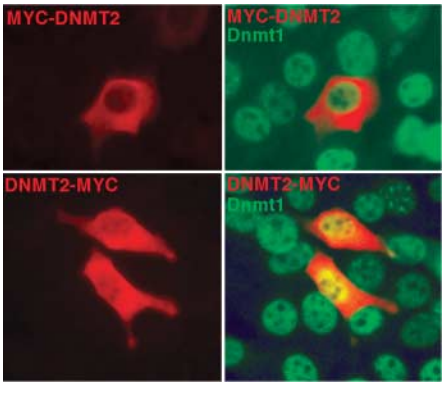

Fig. 1. Cytoplasmic localization of hDNMT2 in NIH3T3 cells. Cells were transiently transfected with hDNMT2 expression constructs that added an N- or C-terminal Myc epitope tag. Immunofluorescence shows localization of hDNMT2 (red) primarily in the cytoplasm, whereas Dnmt1 (green) is exclusively nuclear.

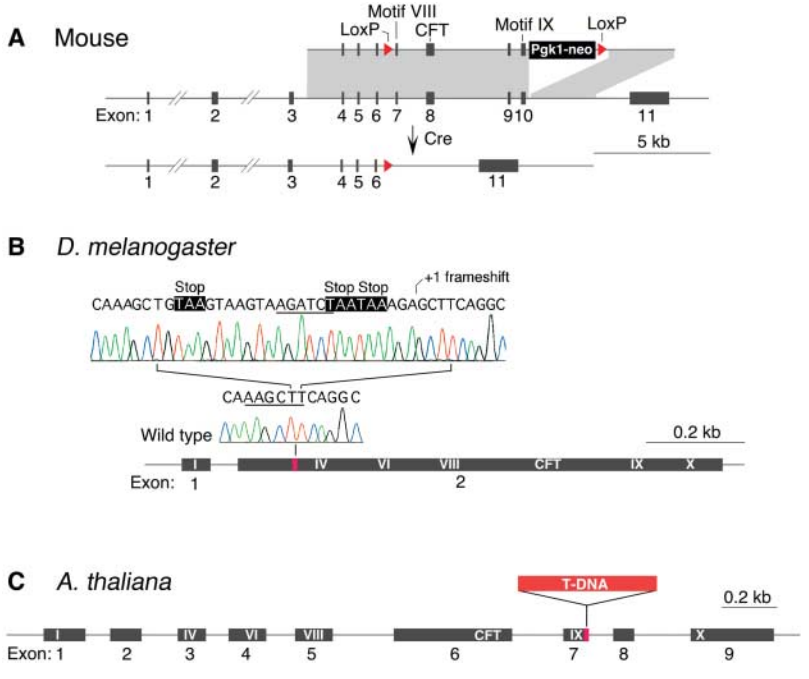

Fig. 2. Mutant alleles of *Dnmt2* homologs in mouse, *D. melanogaster*, and *A. thaliana*. (**A**) loxP sites were introduced into the mouse *Dnmt2* gene by homologous recombination in ES cells, and the indicated deletion was induced by exposure to Cre recombinase (fig. S1). Roman numerals indicate DNA cytosine methyltransferase catalytic motifs. The conserved Cys-Phe-Thr-XX-Tyr-XX-Tyr motif diagnostic of Dnmt2 proteins is indicated by CFT. (**B**) Homologous recombination was used to introduce three in-frame stop codons and a +1 frameshift at the HindIII site in exon 2 of *D. melanogaster dDnmt2*. No wild-type *Mt2/dDnmt2* sequence was present in the homozygous fly stock (fig. S2). (**C**) A large T-DNA insertion 3′ of exon 7 of the *A. thaliana Dnmt2* gene allele truncates the mRNA (fig. S3).

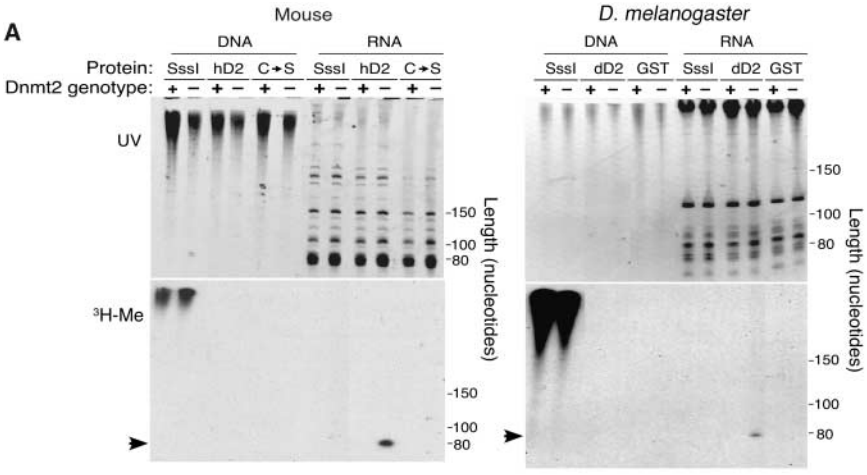

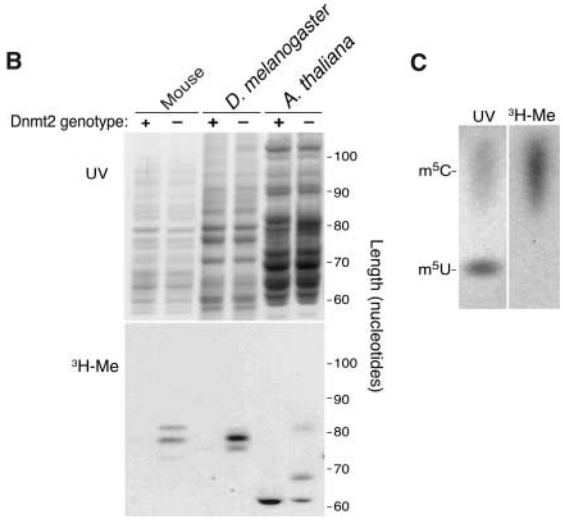

Fig. 3. DNMT2 methylates only a small RNA from DNMT2-deficent tissues. (**A**) Total DNA or RNA from wild-type or *Dnmt2*$^{-/-}$ mice was incubated with ^{3}H-AdoMet and either the bacterial DNA cytosine methyltransferase M.Sss1, His-tagged hDNMT2, or His-tagged hDNMT2 in which Cys^{79} in motif IV was substituted with serine. Nucleic acids were separated by electrophoresis, stained with ethidium bromide, and then prepared for fluorography. No evidence of methylation of DNA by hDNMT2 was seen, but a single small RNA was labeled (arrow) when that RNA originated from Dnmt2$^{-/-}$ mice. Total DNA or RNA from wild-type or *dDnmt2*$^{-/-}$ adult *D. melanogaster* was incubated with M.SssI, glutathione *S*-transferase (GST)-tagged *D. melanogaster* dDnmt2 purified from *E. coli*, or GST alone as on the left-hand gel. Only a small RNA was methylated (arrow). UV, ultraviolet. (**B**) High-resolution analysis of the Dnmt2 target RNA. hDNMT2 was incubated with ^{3}H-AdoMet and total RNA isolated from wild-type and *Dnmt2*$^{-/-}$ mice, *D. melanogaster*, and *A. thaliana*. An additional methylated band with a size of ~68 nucleotides present in RNA from *Dnmt2*$^{-/-}$ *A. thaliana* RNA is likely to represent an additional Dnmt2 substrate in flowering plants. The ~63-nucleotide band in the *A. thaliana* samples is a hDNMT2 substrate even when wild-type RNA is used, which suggests that this RNA species is not methylated in vivo. (**C**) Mouse *Dnmt2*$^{-/-}$ RNA was incubated with hDNMT2 and ^{3}H-AdoMet and hydrolyzed to nucleosides, which were resolved by thin-layer chromatography. The methylated product comigrated with 5-methyl cytosine (m^{5}C).

are required for enzymatic activity (Fig. 2 and figs. S1 to S3).

Strains of mouse, *D. melanogaster*, and *A. thaliana* homozygous for inactivating mutations in *Dnmt2* were viable, fertile, and morphologically indistinguishable from wild-type counterparts. The homozygous *Dnmt2* mutation did not modify the phenotype of mice homozygous for mutations in *Dnmt1*, nor did the homozygous *Dnmt2* mutation modify the phenotypes of *A. thaliana* homozygous for mutations in *drm1* and *drm2* (domains rearranged methyltransferases 1 and 2) or *cmt3* (chromomethylase 3) (*11*). Genomic methylation patterns were not detectably altered in Dnmt2-deficient mouse tissues (fig. S4).

We developed a combined biochemical and genetic approach to address the function of Dnmt2. Purified hDNMT2 was tested for its ability to transfer tritium-labeled methyl groups from the cofactor [^{3}H-*methyl*] S-adenosyl-L-methionine (^{3}H-AdoMet) to genomic DNA and RNA purified from wild-type or *Dnmt2*$^{-/-}$ mice. No DNA methylation was observed (Fig. 3A), but hDNMT2 specifically methylated a small RNA molecule when RNA from *Dnmt2*$^{-/-}$ mouse tissues was the substrate; wild-type RNA from mouse was not labeled (Fig. 3A). This implied that the small RNA molecule was the in vivo target of Dnmt2 and that wild-type RNA is methylated in vivo and cannot serve as substrate for methylation in vitro. Mutation of a key catalytic residue (Cys^{79} in motif IV) (*9*) abolished RNA methyltransferase activity (Fig. 3A). Purified *D. melanogaster* Dnmt2 protein (MT2, hereafter dDnmt2) did not methylate DNA but methylated a small RNA molecule only when that RNA was isolated from *Dnmt2*$^{-/-}$ flies (Fig. 3A).

Dnmt2 was found to have the same function in mammals, flowering plants, and dipteran insects. Purified hDNMT2 methylated one or two RNA molecules of ~80 nucleotides in length when RNA was isolated from *Dnmt2*-deficient mouse, *D. melanogaster*, or *A. thaliana* (Fig. 3, A and B). In all three organisms, hDNMT2 specifically methylated these RNAs only when the RNA was derived from Dnmt2-deficient tissues.

Inspection of the organization of functional groups within the putative active site of hDNMT2 (*4*) indicated that either cytosine or uracil might be the methylation target (*12*). The identity of the modified base was determined by thin-layer chromatography of nucleosides from hydrolysates of RNA labeled with hDNMT2 and ^{3}H-AdoMet. The product of hDNMT2 comigrated with authentic 5-methylcytidine and was clearly resolved from the 5-methyluridine standard (Fig. 3C).

The identity of the RNA substrate was determined by comparison of mass spectra of ribonuclease (RNase) T1 oligonucleotides from the Dnmt2 substrate purified from *Dnmt2*$^{-/-}$ and *Dnmt2*$^{+/+}$ mouse tissues. Matrix-assisted laser desorption/ionization–time-of-flight (MALDI-TOF) mass spectrometry identified a single oligonucleotide that showed a difference of 14 atomic mass units when the wild-type and *Dnmt2*$^{-/-}$ samples were compared, which indicated the loss of a single methyl group (Fig. 4A). Mass spectrometry analysis of this oligonucleotide revealed a hypermodified hexose-queuosine base in the T1 fragment that contained the Dnmt2 target cytosine. Hexose-queuosine has been found in only tRNA^{Tyr} and tRNA^{Asp}, which contain galactosylqueuosine and mannosylqueuosine, respectively; in both cases, the hexose-queuosine is located in the wobble position of the anticodon (*13*, *14*). Tandem mass spectrometry on the T1 fragment that contained the Dnmt2 target cytosine yielded the sequence of the T1 oligonucleotide of the tRNA^{Asp} anticodon loop. Methylation was observed at cytosine 38 of wild-type tRNA^{Asp}, the second nucleotide 3′ of the anticodon, but this position was unmethylated in RNA from Dnmt2-deficient tissues (tables S1 and S2 and fig. S5).

Confirmation that the Dnmt2 target is tRNA^{Asp} was provided by Northern blot analysis of RNA from *Dnmt2*$^{-/-}$ and *Dnmt2*$^{+/+}$ tissues with probes to tRNA^{Asp}. In *Dnmt2*$^{-/-}$ mice, the tRNA substrate showed increased mobility relative to that of the wild type; the mass spectrometry data indicated that this mobility shift was the result of a loss of one methyl group.

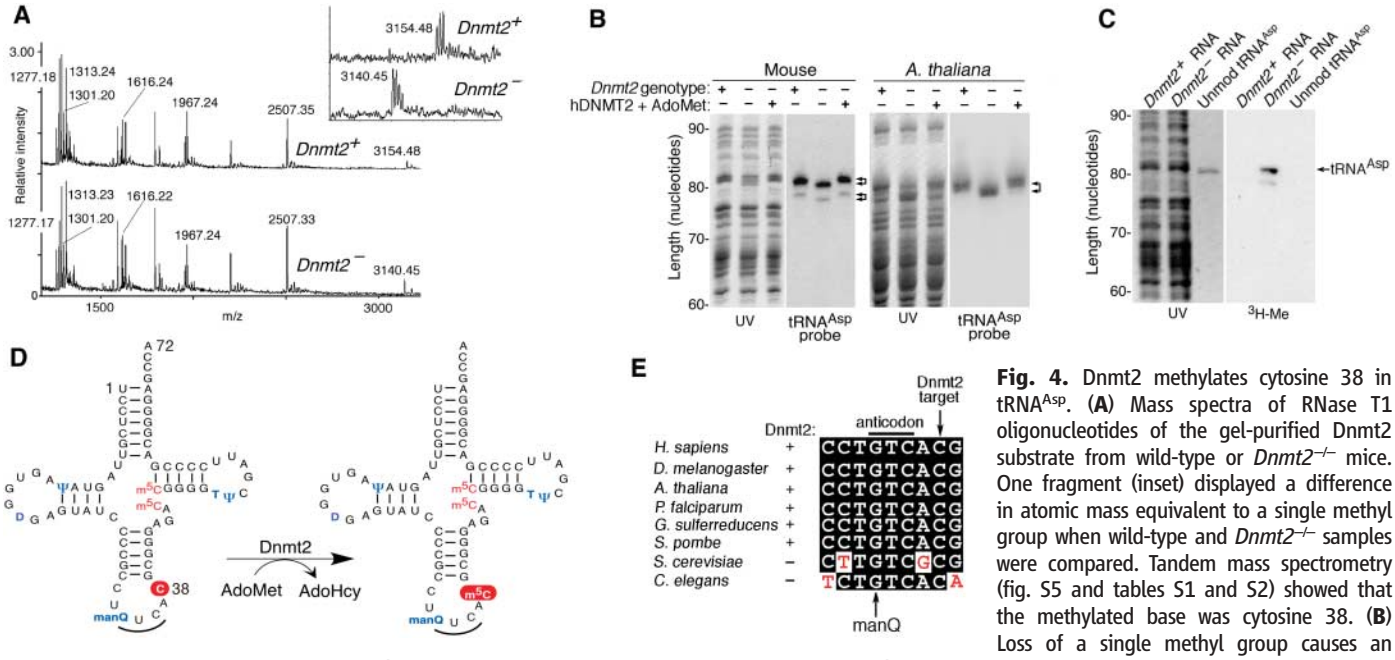

Fig. 4. Dnmt2 methylates cytosine 38 in $tRNA^{Asp}$. (**A**) Mass spectra of RNase T1 oligonucleotides of the gel-purified Dnmt2 substrate from wild-type or *Dnmt2*$^{-/-}$ mice. One fragment (inset) displayed a difference in atomic mass equivalent to a single methyl group when wild-type and *Dnmt2*$^{-/-}$ samples were compared. Tandem mass spectrometry (fig. S5 and tables S1 and S2) showed that the methylated base was cytosine 38. (**B**) Loss of a single methyl group causes an increase in electrophoretic mobility of $tRNA^{Asp}$. Electrophoresis and Northern blot analysis with $tRNA^{Asp}$ probes from mouse and *A. thaliana* confirmed that the target of Dnmt2 is $tRNA^{Asp}$. Identical results were obtained with probes complementary to the 3′ and 5′ ends of $tRNA^{Asp}$. Double arrows indicate the methylation-dependent mobility shift. Dnmt2 in *A. thaliana* has one additional target of ~68 nucleotides in addition to $tRNA^{Asp}$. (**C**) Methylation of $tRNA^{Asp}$ is dependent on preexisting modifications. Unmodified $tRNA^{Asp}$ produced by in vitro transcription was inactive as a hDNMT2 substrate. (**D**) Summary of pattern of modifications of $tRNA^{Asp}$. The mass spectrometry data show that Dnmt2 is required for methylation of position 38 in the anticodon loop of $tRNA^{Asp}$; formation of m^5C at positions 48 and 49 is independent of Dnmt2. Anticodon bases are underlined; mannosylqueuosine is indicated as manQ; other modified nucleosides are shown in blue; pseudouridine is indicated as Ψ; m^5C, in red. (**E**) Sequence alignment of the anticodon loops of $tRNA^{Asp}$. The sequence is invariant among organisms that contain Dnmt2, but base substitutions have occurred at positions adjacent to the target cytosine in $tRNA^{Asp}$ of *S. cerevisiae* and *C. elegans*, whose genomes do not contain a *Dnmt2*-related gene.

Incubation of *Dnmt2*$^{-/-}$ RNA with hDNMT2 and AdoMet restored the wild-type mobility (Fig. 4B). In mouse, the $tRNA^{Asp}$ probe hybridized to two bands of similar mobility, both of which showed a modification-dependent mobility shift (Fig. 4B). These bands are likely to represent populations of differentially modified $tRNA^{Asp}$; heterogeneity of tRNA modification patterns (*15*) and methylation-dependent shifts in electrophoretic mobility of tRNAs (*16*) have been observed. Northern blot analysis of RNA from *A. thaliana* with a $tRNA^{Asp}$ probe revealed a single band that had a Dnmt2-dependent mobility shift, which confirmed that $tRNA^{Asp}$ is the Dnmt2 target in mouse and *A. thaliana* (Fig. 4B). Cytosine 38 had been previously reported to be methylated in $tRNA^{Asp}$ from mouse and *Xenopus laevis* (*14*, *17*) (Fig. 4B). Unmodified $tRNA^{Asp}$ produced by in vitro transcription was not a substrate for DNMT2 (Fig. 4C), which suggests that methylation is guided to cytosine 38 by other modifications; mannosylqueuosine is likely to be involved, because it is unique to $tRNA^{Asp}$.

Analysis of $tRNA^{Asp}$ sequences showed complete conservation of the anticodon loop in species whose genomes encode Dnmt2 homologs, but the $tRNA^{Asp}$ anticodon loops in *Caenorhabditis elegans* and *Saccharomyces cerevisiae*, which lack Dnmt2 homologs, have diverged (Fig. 4E). The bacterium *Geobacter sulferreducens* contains a Dnmt2 homolog, and the $tRNA^{Asp}$ anticodon loop of this organism is identical to that of Dnmt2-containing eukaryotes. These findings indicate coevolution of Dnmt2 and the anticodon loop of $tRNA^{Asp}$. The strong conservation of Dnmt2 across divergent taxa indicate that it is under positive selection and suggests that Dnmt2 increases fitness under unidentified sources of stress or has an incremental effect on fitness that is not apparent under laboratory conditions.

The data shown here indicate that Dnmt2 methylates an RNA, even though the sequence and the order of catalytic motifs of Dnmt2 are characteristic of DNA rather than RNA methyltransferases (*18*, *19*). Methylation of $tRNA^{Asp}$ by Dnmt2 requires information beyond the RNA sequence, and structural information is involved in target selection by other RNA methyltransferases (*20*, *21*). Indirect sequence recognition is also a feature of eukaryotic DNA cytosine methyltransferases (*1*), whereas bacterial restriction methyltransferases have innate sequence specificity that determines the structure of genomic methylation patterns in these organisms [reviewed in (*22*)]. This raises the possibility that eukaryotic DNA cytosine methyltransferases were derived from an ancestral Dnmt2-like RNA methyltransferase rather than prokaryotic restriction DNA methyltransferases, which could explain the profound differences in mechanisms of target selection by DNA cytosine methyltransferases of prokaryotes and eukaryotes (*1*).

References and Notes

1. M. G. Goll, T. H. Bestor, *Annu. Rev. Biochem.* **74**, 481 (2005).
2. C. R. Wilkinson, R. Bartlett, P. Nurse, A. P. Bird, *Nucleic Acids Res.* **23**, 203 (1995).
3. J. A. Yoder, T. H. Bestor, *Hum. Mol. Genet.* **7**, 279 (1998).
4. A. Dong *et al.*, *Nucleic Acids Res.* **29**, 439 (2001).
5. J. Posfai, A. S. Bhagwat, G. Posfai, R. J. Roberts, *Nucleic Acids Res.* **17**, 2421 (1989).
6. M. Okano, S. Xie, E. Li, *Nucleic Acids Res.* **26**, 2536 (1998).
7. H. Leonhardt, A. W. Page, H. U. Weier, T. H. Bestor, *Cell* **71**, 865 (1992).
8. K. E. Bachman, M. R. Rountree, S. B. Baylin, *J. Biol. Chem.* **276**, 32282 (2001).
9. D. V. Santi, C. E. Garrett, P. J. Barr, *Cell* **33**, 9 (1983).
10. J. M. Alonso *et al.*, *Science* **301**, 653 (2003).
11. M. G. Goll *et al.*, unpublished data.
12. M. Sprinzl, K. S. Vassilenko, *Nucleic Acids Res.* **33**, D139 (2005).
13. G. D. Johnson, I. L. Pirtle, R. M. Pirtle, *Arch. Biochem. Biophys.* **236**, 448 (1985).
14. Y. Kuchino, N. Shindo-Okada, N. Ando, S. Watanabe, S. Nishimura, *J. Biol. Chem.* **256**, 9059 (1981).
15. H. Taniguchi, N. Hayashi, *Nucleic Acids Res.* **26**, 1481 (1998).
16. D. Mangroo, P. A. Limbach, J. A. McCloskey, U. L. RajBhandary, *J. Bacteriol.* **177**, 2858 (1995).
17. E. Haumont, K. Nicoghosian, H. Grosjean, R. J. Cedergren, *Biochimie* **66**, 579 (1984).

18. C. Gustafsson, R. Reid, P. J. Greene, D. V. Santi, *Nucleic Acids Res.* **24**, 3756 (1996).
19. M. Y. King, K. L. Redman, *Biochemistry* **41**, 11218 (2002).
20. P. G. Foster, C. R. Nunes, P. Greene, D. Moustakas, R. M. Stroud, *Structure* **11**, 1609 (2003).
21. T. T. Lee, S. Agarwalla, R. M. Stroud, *Cell* **120**, 599 (2005).
22. X. Cheng, R. J. Roberts, *Nucleic Acids Res.* **29**, 3784 (2001).
23. We thank K. Anderson and M. Damelin for comments on the manuscript; X. Cheng for helpful discussions; and B. Berkovits, S. Chen, B. Erlanger, A. Getz, A. Kljuic, C. Köhrer, N. Papavasiliou, K. Politi, and U. RajBhandary for advice and assistance. Supported by grants from the NIH and the Danish Natural Science Research Council.

Supporting Online Material
www.sciencemag.org/cgi/content/full/311/5759/395/DC1
Materials and Methods
Figs. S1 to S5
Tables S1 and S2

5 October 2005; accepted 20 December 2005
10.1126/science.1120976

fwww.sciencemag.org/cgi/content/full/311/5759/395/DC1

Supporting Online Material for

Methylation of tRNA^{Asp} by the DNA Methyltransferase Homolog Dnmt2

Mary Grace Goll, Finn Kirpekar, Keith A. Maggert, Jeffrey A. Yoder, Chih-Lin Hsieh, Xiaoyu Zhang, Kent G. Golic, Steven E. Jacobsen, Timothy H. Bestor*

*To whom correspondence should be addressed. E-mail: THB12@Columbia.edu

Published 20 January 2006, *Science* **311**, 395 (2006)
DOI: 10.1126/science.1120976

This PDF file includes:

Supporting Online Material

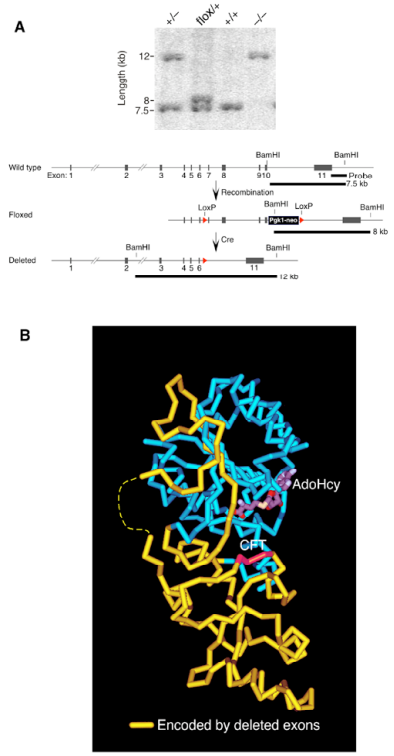

Supplementary Fig. S1. Confirmation of the genotype of *Dnmt2*$^{-/-}$ mice. (**A**) Southern blot showing excision of the targeted floxed *Dnmt2* gene in BamHI-digested genomic DNA. An additional BamHI site in the neomycin cassette results in an 8Kb fragment after introduction of loxP sites (flox). After exposure to Cre recombinase excision of the floxed allele results in loss of BamHI sites and a 12kb fragment. (**B**) Crystal structure of hDNMT2 in which the segment of the protein deleted by loxP recombination is highlighted in yellow; the CFTXXYXXY motif, which is also deleted, is shown in red.

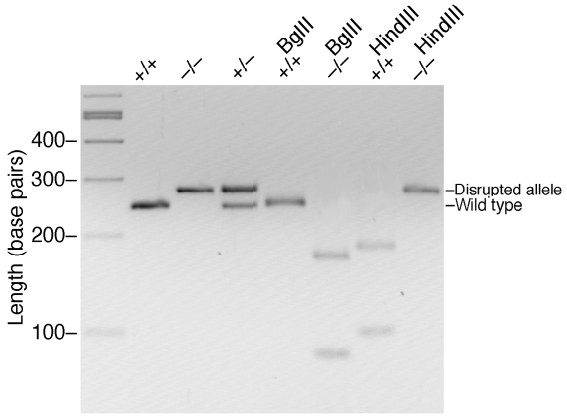

Supplementary Fig. S2. Confirmation of genotype of *dDnmt2*$^{-/-}$ *D. melanogaster.* (**A**) PCR analysis shows lack of wildtype *dDnmt2* sequence in mutant DNA. The wildtype allele contains a HindIII site, which was deleted after homologous recombination; the mutant allele contains a BglII site not present in the wildtype. The size and fragment patterns confirm the sequence shown in Fig. 2B and show that no wildtype *dDnmt2* sequence is present in the mutant flies used in this study.

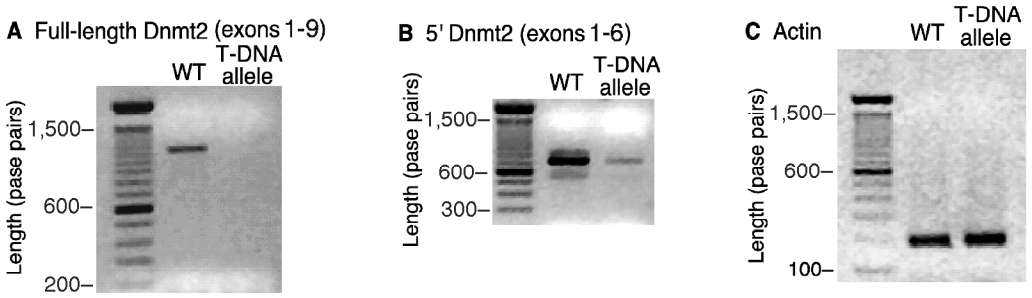

Supplementary Fig. S3. Confirmation of Dnmt2 disruption in *A. thaliana* by RT-PCR (**A**) RT-PCR using primers in exons 1 and 9 of *A. thaliana* Dnmt2 indicate that full length Dnmt2 mRNA is not present. (**B**) RT-PCR using primers in exon 1 and 6 indicate that there is a severe decrease in Dnmt2 mRNA 5' of the T-DNA insertion. This truncated mRNA lacks coding sequence for DNA methyltransferase motif X. (**C**) RT-PCR control with primers complementary to the actin mRNA.

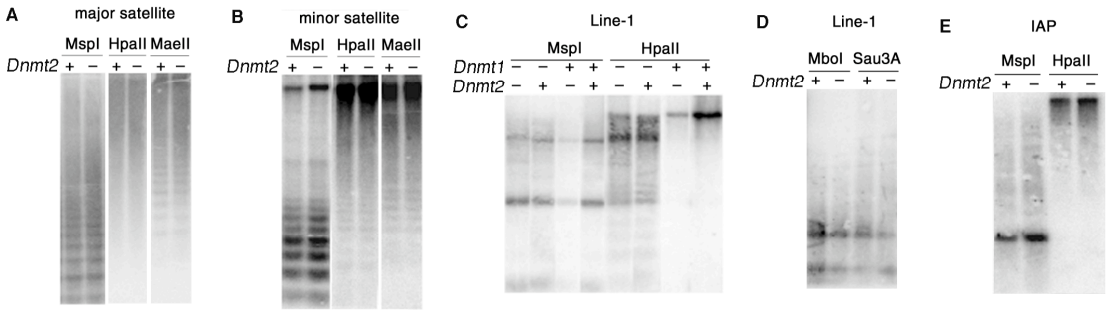

Supplementary Fig S4. Representative Southern blots showing that DNA methylation patterns are unaffected in *Dnmt2*$^{-/-}$ mice. (**A-B**) Methylation sensitive Southern blots were performed on DNA from purified from wildtype and *Dnmt2*$^{-/-}$ mice after digestion with the methylation sensitive restriction enzymes HpaII (CCGG) or MaeII (ACGT) and the methylation insensitive HpaII isoschizomer MspI. Blots were probed for major satellite sequences (**A**) or minor satellite sequences (**B**). (**C**) Methylation sensitive Southern blot on DNA purified from *Dnmt2*$^{-/-}$ mice and *Dnmt2*$^{-/-}$ *Dnmt1*$^{N/N}$ mice digested with HpaII or MspI hybridized to a Line-1 probe (**D**) Methylation sensitive Southern blot of DNA from wildtype and *Dnmt2*$^{-/-}$ mice digested with the methylation sensitive enzyme Sau3A (GATC) and its methylation insensitive isoschizomer MboI hybridized to a Line-1 probe. (**E**) Methylation sensitive Southern blot with a probe to the Interstitial-A particle (IAP) transposon long terminal repeat (LTR) after digestion with HpaII or MspI.

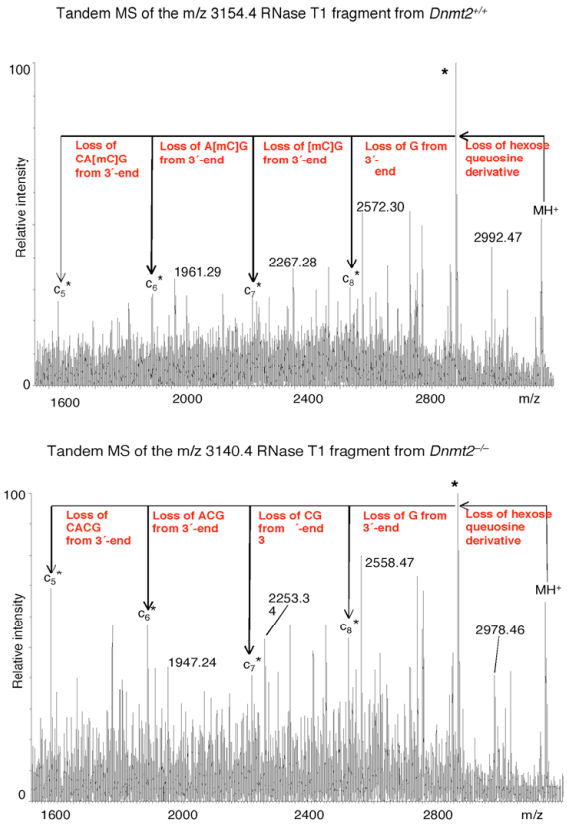

Supplementary Fig. S5. Position 38 of $tRNA^{Asp}$ is modified by DNMT2. (A) Tandem MS of the m/z 3154.4 RNase T1 fragment from $tRNA^{Asp}$ purified from wildtype mouse tissues. Peaks corresponding to loss of 3' nucleotides are indicated as peaks C_5-C_8. Peaks corresponding to loss of 5' nucleotides are indicated by their m/z. Interpretation of all peaks is included in Table S2. (B) Tandem MS of the m/z 3140.4 RNase T1 fragment from $tRNA^{Asp}$ purified from *Dnmt2*$^{-/-}$ mouse tissues. The m/z of C_8 shows a difference corresponding to one methyl group between wildtype and *Dnmt2*$^{-/-}$ samples with loss of the 3' most G. The m/z of C_7 indicates loss of m^5C from the *Dnmt2*$^{+/+}$ sample and loss of C from the *Dnmt2*$^{-/-}$ sample .

From-To	M/Z calculated	Sequence	M/Z observed	Sequence by tandem MS
1-6	1953.20	PO_4-UCCUCG-PO_4	1967.24	PO_4-UCCUCG^m-PO_4
7-10	1287.16	UUAG-PO_4	1301.20	UUA^{m}G-PO_4
11-15	1616.21	UAUAG-PO_4	1616.22	UAUAG-PO_4
16-17	652.08	UG-PO_4	n.o.	-
18-18	346.05	G-PO_4	n.o.	-
19-20	652.08	UG-PO_4	n.o.	-
21-22	675.11	AG-PO_4	n.o.	-
23-30	2507.32	UAUCCCCG-PO_4	2507.33	UAUCCCCG-PO_4 (1)
31-34	**1262.16**	**CCUG-PO_4**	**3140.45**	**CCUXXCACG-PO_4+ hexose-queousine**
35-39	**1591.22**	**UCACG-PO_4**		

40-41	651.10	CG-PO_4	n.o.	-
42-42	346.05	G-PO_4	n.o.	-
43-43	346.05	G-PO_4	n.o.	-
44-45	675.11	AG-PO_4	n.o.	-
46-49	1285.19	ACCG-PO_4	1313.23	AC^mC^mG-PO_4
50-50	346.05	G-PO_4	n.o.	-
51-51	346.05	G-PO_4	n.o.	-
52-52	346.05	G-PO_4	n.o.	-
53-56	1263.15	UUCG-PO_4	1277.17	U^mUCG-PO_4
57-64	2507.32	AUUCCCCG-PO_4	2507.33	AUUCCCCG-PO_4 (1)
65-67	980.15	ACG-PO_4	980.15	Not performed
68-68	346.05	G-PO_4	n.o.	-
69-69	346.05	G-PO_4	n.o.	-
70-70	346.05	G-PO_4	n.o.	-
71-72	595.14	AG-OH	n.o.	-

Supplementary Table S1. T1 fragments identified from the purified Dnmt2 substrate RNA correspond to $tRNA^{Asp}$. The anticodon loop containing the Dnmt2 target cytosine is indicated in bold. RNAse T1 cleaves RNA 3' of G residues. T1 does not cleave at mannosylqueousine and as a result, predicted fragments 31-34 and 35-39 appear as a single oligonucleotide by mass spectrometry. n.o. indicates that the mass spectra of the T1 fragment was not obtained due to its small size. (1) These two fragments are isobaric. The tandem MS data suggested two species, one starting with a U and one with an A, but an otherwise identical fragmentation patterns. There was no evidence of a Dnmt2-dependent change of mass in these fragments. The sequence of mouse $tRNA^{Asp}$ appears in Fig 4D.

Tandem MS of the m/z 3154.4 RNase T1 fragment from Dnmt2$^{+/+}$ tRNA

M/Z	Interpretation	Comment
3154.45	MH^+	Singly protonated parent ion for the tandem MS experiment.
2992.47	Hexose loss from MH^+	Loss of 162 is well-known diagnostic signal for hexose loss in tandem MS of carbohydrates.
2877.41	Loss of queuosine-derivative from MH^+	Loss of 277 corresponds to the dominating fragmentation site for queuosine derivatives [1]. Marked * in the spectrum.
2572.30	y_8*	Loss of C nucleotide from the 5´-end of the *-marked species.
2532.32	c_8*	Loss of G nucleotide from the 3´-end of the *-marked species.
2267.28	y_7*	Loss of CC di-nucleotide from the 5´-end of the *-marked species.
2213.24	c_7*	Loss of [C+methyl]G di-nucleotide from the 3´-end of the *-marked species. Reveals the Dnmt2 methylation site.
1961.29	y_6*	Loss of CCU tri-nucleotide from the 5´-end of the *-marked species.
1884.20	c_6*	Loss of A[C+methyl]G tri-nucleotide from the 3´-end of the *-marked species.
1579.15	c_5*	Loss of CA[C+methyl]G tri-nucleotide from the 3´-end of the *-marked species.

Tandem MS of the m/z 3140.4 RNase T1 fragment from Dnmt2$^{-/-}$ tRNA

M/Z	Interpretation	Comment
3140.43	MH^+	Singly protonated parent ion for the tandem MS experiment.
2978.46	Hexose loss from MH^+	Loss of 162 is well-known diagnostic signal for hexose loss in tandem MS of carbohydrates.
2863.57	Loss of queuosine-derivative from MH^+	Loss of 277 corresponds to the dominating fragmentation site for queuosine derivatives [1]. Marked * in the spectrum.
2558.47	y_8*	Loss of C nucleotide from the 5´-end of the *-marked species.
2518.31	c_8*	Loss of G nucleotide from the 3´-end of the *-marked species.
2253.34	y_7*	Loss of CC di-nucleotide from the 5´-end of the *-marked species.
2213.35	c_7*	Loss of CG di-nucleotide from the 3´-end of the *-marked species. Loss is [C+methyl]G in Dnmt2+/+ sample

1947.24	y_6*	Loss of CCU tri-nucleotide from the 5´-end of the *-marked species.
1884.31	c_6*	Loss of ACG tri-nucleotide from the 3´-end of the *-marked species.
1579.20	c_5*	Loss of CACG tri-nucleotide from the 3´-end of the *-marked species.

Supplementary Table S2. Interpretation of spectra from Fig. S5.

Materials and Methods

Disruption of Dnmt2 Genes

The mouse genomic library 129SVter DNA in λFIXII (Stratagene) was screened with a Dnmt2 cDNA probe and a clone encoding exons 4 through 11 was identified. The synthetic oligo GGTACCATAACTTCGTATAATGTATGCTATACGAAGTTATGTTTAAACGGTACC containing a loxP site was introduced into the unique KpnI site upstream of exon 7. A second LoxP site and the neomycin cassette from plasmid pLTNL (gift of Thomas Ludwig) was introduced into the AflII site downstream of the exon 10. Initial screening of the mouse ES cells to confirm proper integration of the portion of the targeting cassette was performed by Southern blot using a 460 bp PCR probe amplified using primers GAACTCACACGGGCATTGTA and GGCTCATGATTAGTCTGCTCAA. Proper targeting of the 5' loxP site was confirmed in 3' positive clones by PCR using primers AGAAGCCTGTGGCTTTCAGT and CCCTACAATCGTTTATTTTCCAA. Properly targeted heterozygous ES cells were injected into blastocysts and chimeric mice identified. After germline transmission, heterozygous mice were crossed to mice expressing Cre recombinase under the *hsp70* promoter. Proper recombination between LoxP sites was assessed by Southern blotting and mice were crossed to homozygosity. PCR amplification and direct sequencing of the product confirmed excision of the antibiotic resistance cassette and *Dnmt2* exons 7-10.

D. melanogaster Dnmt2 mutant flies were created by introducing the oligonucleotide AGCTGTAAGTAAGTAAGATCTAATAAAG into the endogenous HindIII site 3' of motif IV according to (*2*). The resulting truncation results in a protein of 67 amino acids. Genotyping of flies was achieved by PCR across the boundary of the targeted HindIII site using primers GTTTATGCGCACAATTACGG and GAAACCCTTGACGTTTTCCA. PCR products were gel purified and sequenced in both directions. No evidence of any wild type *dDnmt2* sequence was found in mutant flies homozygous for the mutant allele.

The *A. thaliana* T-DNA insertion mutant documented polymorphism SALK_1366 was obtained from the *Arabidopsis* information resource (TAIR) under accession number 1005061271 (*3*). RT-PCR primers were ATGGCGGAACAAGAATTACAGA and TCAAGAATCGAATAGATACCGAA for full length Dnmt2 mRNA and ACACTACTTGGCTCGCCATCAA and ATGGCGGAACAAGAATTACAGA for exons 1-6.

Protein Expression and Purification

Human RGS6XHis tagged Dnmt2 was expressed and purified as in (*4*). *Drosophila* dDnmt2 cDNA was obtained from Open Biosystems (cat EDM1133-6873739) and was cloned into pGEX2T in frame with an N-terminal GST tag. *Drosophila* dDnmt2 protein was expressed in *E. coli* (McrBC deficient strain ER2488) and soluble recombinant protein was purified on GST agarose (Molecular Probes) according to manufacturers instructions.

Immunocytochemistry

NIH3T3 cells were transiently transfected with the use of lipofectamine (Invitrogen). Expression plasmids consisted of hDNMT2 fused to an N or C terminal MYC epitope tag. Expression required sequences to be cloned downstream of the γ-globin intron 2. At 24 h post transfection cells were fixed with formaldehyde and viewed by

immunoflourescence using the anti MYC antibody 9E10 (Biosource) and polyclonal rabbit anti-Dnmt1 antibody (anti-PATH52) (4, 5) as primary antibodies.

Methyltransferase assay

5 μg of RNA or DNA purified from mouse liver was incubated with 40 ng of purified protein, 1 uCi [^{3}H] S-Adenosyl-L-methionine (15 Ci mmol^{-1}; Amersham) and 5 units of RNaseIN (Promega). Samples were incubated 2 h at 37° in 20mM Tris-HCl (pH 7.4), 0.5 mM DTT, 2 mM EDTA, 50 mM KCL, 5% glycerol. After methylation reactions were complete, DNA was subjected to digestion with MboI to reduce fragment size. Samples were phenol extracted, ethanol precipitated, resuspended in formamide, and run on a 12% denaturing poly acrylamide gel. Fluorographic detection of tritium signal was achieved by soaking the gel in 2 M sodium salicylate in 45% methanol-10% acetic acid for 1 h. Gels were dried and exposed to Biomax film (Kodak) at –70° C. For *D. melanogaster*, experimental conditions were the same as above except that 2 μg of DNA or 20 μg of total RNA from freshly eclosed adult flies was used as substrate. M. SssI was purchased from New England Biolabs (NEB).

Thin layer chromatography

Total RNA from *Dnmt2*$^{-/-}$ mice was incubated with hDNMT2 and ^{3}H-AdoMet for 2 h. RNA was then passed over an RNA QuickSpin column (Roche). Nucleosides were generated by incubation first with P1 nuclease (100 μg/ ml) in 30 mM sodium acetate pH 5.3, 0.1 mM $ZnCl_2$ at 60° C for 1h, followed by 5 units calf alkaline phosphatase (NEB) for 1 h at 37° C in the provided buffer. Mononucleosides were separated by thin layer chromatography on cellulose plates developed in isobutyric acid-ammonium hydroxide-0.1 M EDTA (100: 60: 1.6) (*5*). Ribothymidine standard (Mann Research laboratories) was a kind gift of B. Erlanger (Columbia University). 5-methylcytidine was purchased from Sigma. RNA was visualized by UV shadowing and the position of the standards was documented, tritium signals on the same plate were then visualized by fluorography according to (*6*).

Mass spectrometry

Total RNA purified from wild type and *Dnmt2*$^{-/-}$ mouse tissues was run on a denaturing polyacrylamide gel for 22 h and visualized by ethidum bromide staining. The single band that shows a change in mobility between wild type and *Dnmt2*$^{-/-}$ RNA was excised and eluted in 2 M ammonium acetate. The digestion mixture contained approximately 1 pmol/μl Dnmt2 substrate tRNA, 50 mM 3-hydroxypicolinic acid and 100 u/μl RNase T1 (USB). Digestion was performed for 4 hours at 37° C. These digestion conditions produced almost exclusively 2´-3´ cyclic phosphate digestion products. Samples for mass spectrometry were prepared by mixing 1 μl of tRNA digestion mixture with 0.7 μl of 0.5 M 3-hydroxypicolinic acid in 50% acetonitrile and approximately 0.1 μl of ammonium-loaded cation exchange beads, after which the sample was left to air-dry at room temperature. MALDI mass spectrometry was performed on a Perseptive Voyager STR MALDI instrument detecting positive ions in reflector Time of Flight mode. Spectrum processing was done with the producer-supplied software using internal calibration. Tandem mass spectrometry was done on a Micromass MALDI Q-TOF Ultima instrument in positive ion mode using the same sample preparation as above. Details may be found in (*7*).

Northern Blots

Total RNA was run on a 12% denaturing polyacrylamide gel at 800V for 22h and stained with ethidium bromide. RNA was transferred to a nylon membrane by semidry electrophoretic transfer. Membranes were hybridized and washed using end labeled probes as in (*8*), except washes were carried out at 55° C. Probe sequences were as follows: mouse $tRNA^{Asp}$ probes, CTCCCCGTCGGGGAATTGAA and GATACTACCACTATACTAACGAGGA; *A. thaliana* $tRNA^{Asp}$ probe: ATACTTACCACTATACTACAACGAC, *D. melanogaster*: GATACTAACCACTATACTATCGAGGA and CTCCCCGACGGGGAATTGAA.

In vitro transcription of mouse $tRNA^{Asp}$

The $tRNA^{Asp}$ DNA template was created using the primers TGGCGCCCCGTCGGGGAATTGAACCCCGGTCTCCCGC and AAGCTTAATACGACTCACTATAGCCTCGTTAGTATAGTGGT and a template oligonucleotide corresponding to positions 1 to 52 of mouse $tRNA^{Asp}$. PCR replaces T at position 1 of $tRNA^{Asp}$ with a G to allow for T7 transcription and position 71 A with a C to maintain the hairpin structure of tRNA as in (*9*). Reactions were treated with DNAse and run on a denaturing polyacrylamide gel with size standards. The largest T7 transcript, corresponding to full-length $tRNA^{Asp}$ was gel purified, eluted and tested for its ability to accept a methyl group from ^{3}H-AdoMet as described previously.

Southern Blot Probes

An oligo probe corresponding to the sequence AACAGTGTATATCAATGAGTTACAATGAG was used to probe minor satellite sequences. For the major satellite, a 250 bp insert was excised from pMR196 (*10*). The L1 5-UTR probe was amplified according to (*11*). The IAP probe was as described in (*12*).

References

1. D. W. Phillipson *et al.*, *J Biol Chem* **262**, 3462 (1987).
2. Y. S. Rong, K. G. Golic, *Science* **288**, 2013 (2000).
3. J. M. Alonso *et al.*, *Science* **301**, 653 (2003).
4. A. Dong *et al.*, *Nucleic Acids Res* **29**, 439 (2001).
5. H. Rogg, R. Brambilla, G. Keith, M. Staehelin, *Nucleic Acids Res* **3**, 285 (1976).
6. W. M. Bonner, J. D. Stedman, *Anal Biochem* **89**, 247 (1978).
7. J. Mengel-Jorgensen, F. Kirpekar, *Nucleic Acids Res* **30**, e135 (2002).
8. C. Kohrer, E. L. Sullivan, U. L. RajBhandary, *Nucleic Acids Res* **32**, 6200 (2004).
9. V. Perret *et al.*, *Biochimie* **72**, 735 (1990).
10. D. F. Pietras *et al.*, *Nucleic Acids Res* **11**, 6965 (1983).
11. K. P. Lu, K. S. Ramos, *J Biol Chem* **278**, 28201 (2003).
12. C. P. Walsh, J. R. Chaillet, T. H. Bestor, *Nat Genet* **20**, 116 (1998).